福昕PDF编辑器

• 永久　• 轻巧　• 自由

升级会员　　批量购买

永久使用

无限制使用次数

极速轻巧

超低资源占用，告别卡顿慢

自由编辑

享受Word一样的编辑自由

扫一扫，关注公众号

福昕PDF编辑器

• 永久　• 轻巧　• 自由

升级会员　　批量购买

永久使用

无限制使用次数

极速轻巧

超低资源占用，告别卡顿慢

自由编辑

享受Word一样的编辑自由

扫一扫，关注公众号

Fast and robust small infrared target detection using absolute directional mean difference algorithm

Saed Moradi, Payman Moallem*, Mohamad Farzan Sabahi

Department of Electrical Engineering, Faculty of Engineering, University of Isfahan, Isfahan, Iran

Abstract

Infrared small target detection in an infrared search and track (IRST) system is a challenging task. This situation becomes more complicated when high gray-intensity structural backgrounds appear in the field of view (FoV) of the infrared seeker. While the majority of the infrared small target detection algorithms neglect directional information, in this paper, a directional approach is presented to suppress structural backgrounds and develop more effective detection algorithm. To this end, a similar concept to the average absolute gray difference (AAGD) is utilized to construct a novel directional small target detection algorithm called absolute directional mean difference (ADMD). Also, an efficient implementation procedure is presented for the proposed algorithm. The proposed algorithm effectively enhances the target area and eliminates background clutter. Simulation results on real infrared images prove the significant effectiveness of the proposed algorithm. .

Keywords: small infrared target detection, directional mean difference, average absolute gray difference, structural background

1. Introduction

Infrared imaging plays a vital role in a wide range of applications in remote sensing [1, 2] and long-distance target detection is of great importance for surveilance applications. In this filed, small infrared target detection remains a major challenge despite advances in infrared detector technology and image processing techniques [3]. This challenge becomes more critical when the long-distant target is embedded in a noisy and complicated background [4].

There are too many researches in the literature which are dedicated to the small infrared target detection field. Background subtraction methods like as max-mean and max median [5], morphology opening [6] are the fast and low complexity methods. Although, these methods have a high false-alarm rate due to imperfect background estimation. The other type of small target detection algorithms

*Corresponding author.
Email address: p_moallem@eng.ui.ac.ir (Payman Moallem)

simultaneously enhances the target area and suppresses the background clutter. Laplacian of Gaussian (LoG) scale-space was proposed to distinguish the target from background clutter by maximum selection in scale dimension [7]. While this method is able to detect low contrast point-wise target, the second derivative part of the filter boosts background noise. Local contrast measure (LCM) [8] has a good ability to enhance target region. However, LCM amplifies the single-pixel salt noise and increases the number of false-alarms. Additionally, the high-intensity background clutters are also intensified in the output image. Average absolute gray difference (AAGD) algorithm [9] effectively suppresses background noise (using local averaging) and enhances target area (by adopting local contrast). Since this algorithm can be easily implemented via local averaging and subtraction operators, the AAGD algorithm has low computational complexity and is suitable for real-time practical applications. However, AAGD faces major problem when the infrared scenario contains high intensity edges and structural background clutter. In this situation, AAGD returns false responses as true target area. In multi-scale patch-based contrast measure (PCM) [10] after dividing each interesting area into nine patches, dissimilarity between the surrounding patches and the central one are calculated. After multiplying directional dissimilarities and minimum selection among the results, the final output is obtained. While the directional approach utilized in this method is remarkable, However, by multiplying the directional dissimilarities all efforts would be vain. Note that, multiplying different directional information is the only data fusion which has been utilized in the literature.

In order to develop robust and effective small target detection algorithm and resolve the aforementioned issues, in this paper, a directional approach is presented and adopted into the AAGD algorithm. The rest of this paper is organized as follows: In the next section the related background and motivation is discussed briefly. The section III is dedicated to the proposed small target detection algorithm followed by simulation results in the section IV. Finally, The paper is concluded in the section V.

2. Background and motivation

2.1. Average absolute gray difference algorithm

Average absolute gray difference (AAGD) algorithm is one of the most effective small target detection algorithms in noisy scenarios [9]. Since this algorithm utilizes local averaging, it has good capability to eliminate background noise. The target enhancement mechanism in this method relies on the existing contrast between the target region and local background area. This algorithm is utilizing two nested windows which are sliding pixel by pixel. The difference between the average values of the internal window (Φ) and the external window (Ω) is used to construct saliency map. The saliency map

construction in AAGD algorithm can be mathematically formulated as

$$AAGD = \left| \frac{1}{N_\Phi} \sum_{(s,t)\in\Phi} I(s,t) - \frac{1}{N_\Omega} \sum_{(p,q)\in\Omega} I(p,q) \right|^2, \quad (1)$$

where $I(x,y)$, N_Φ and N_Ω stand for the pixel intensity at position (x,y), the total number of pixels contained in the set Φ and the total number of pixels contained in the set Ω, respectively.

AAGD algorithm has a good ability to enhance low contrast target and eliminate background noise. However, when the infrared scenario contains high-intensity edges and structural background clutter, non-target areas are also intensified. Also, while target area always has positive contrast, AAGD returns strong response no matter whether the contrast of an interested region is positive or negative [11].

To address the aforementioned issues and overcome deficiencies of the AAGD algorithm, a directional approach is utilized here to achieve better clutter rejection and background suppression capability. The proposed approach is adopted in the AAGD algorithm and a new small infrared target detection algorithm called absolute directional mean difference (ADMD) is developed. The following section describes the proposed algorithm.

3. The proposed algorithm

While the directional filter design concept was presented and investigated in small infrared target detection field of study [12, 13, 14], the lack of proper data fusion strategy avoids robust small target detection. As mentioned in the introduction section, multiplication is the only fusion strategy which has been investigated. Using multiplication to obtain final output from directional filters (similar to what proposed by [10]) will put all efforts in vain. In order to address this issue and avoiding data loss, the fusion strategy is modified in a way to improve clutter rejection ability.

Generally, infrared targets have a positive local contrast which means that the target area is brighter than local background in all directions (neglecting special cases like the situation which target is close to high gray intensity background clutter). Considering this fact into account, it appears that utilizing all information from the all directional filters effectively can suppress high-intensity structural background. As shown in Fig. 1, a small infrared target (red rectangle) has positive contrast in all directions while a high-intensity edge (yellow rectangle) does not have a such property. Hence, using the minimum value of the directional AAGD algorithm will effectively enhance false-alarm suppression ability. The following procedure describes the saliency map construction of the proposed method.

As depicted in Fig. 2, two nested windows are assigned for each pixel (i,j) in the input image. The internal one, u, denotes the target window and its size is related to the small infrared target size

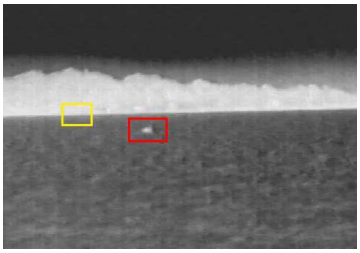

Figure 1: Target and high intensity edge in real infrared scenario

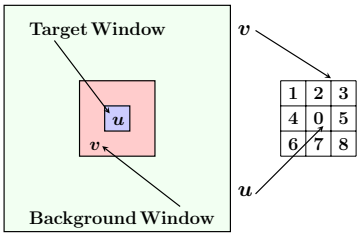

Figure 2: Target and background window

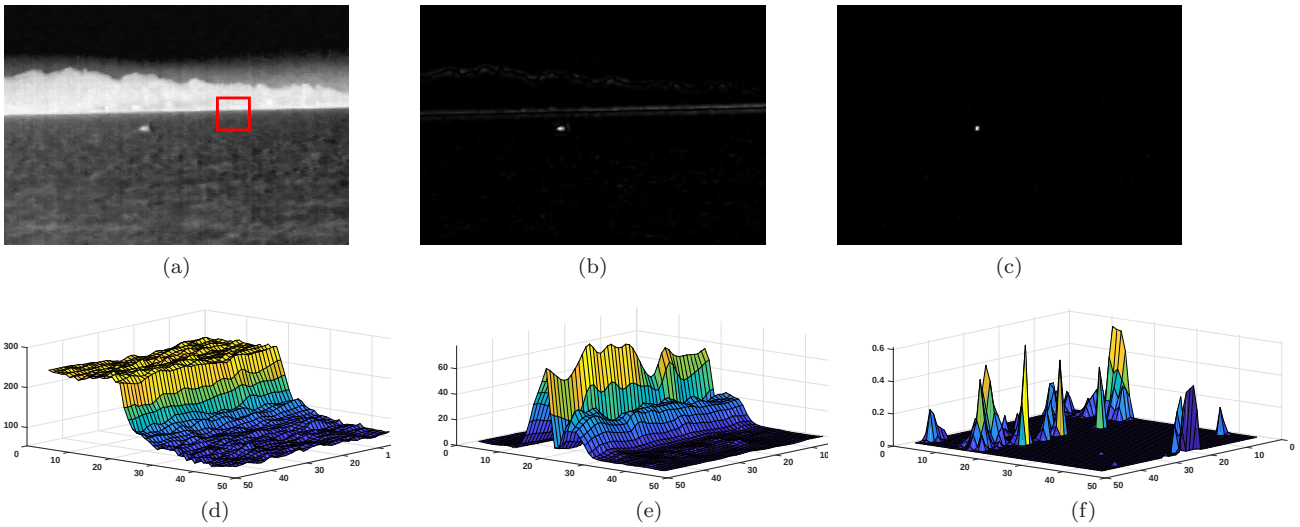

Figure 3: The output response of the AAGD, as well as the proposed algorithm, to a sharp edge: **a)** original input image, **b)** the filtering result of the AAGD algorithm, **c)** the filtering result of the proposed algorithm, **d)** 3-D surface of the red rectangle in the input image, **e)** 3-D surface of the red rectangle in the filtering result of the AAGD algorithm, **f)** 3-D surface of the red rectangle in the filtering result of the proposed algorithm. Note that, the gray intensity of all images are normalized to $[0-255]$ interval.

(typically smaller than 9×9). The external window, v, stands for local background window and its size is 3 times of the size of the target window. As shown in the figure, the external window is divided to 9 equal cells (obviously the cell 0 is the target window u). The average intensity of the pixels of the cell k is denoted by m_k and calculated as follows:

$$m_k(i,j) = \frac{1}{N_{cell}} \sum_{(s,t)\in cell_k} I^k(s,t) \qquad i = 0,1,\ldots,8 \tag{2}$$

where, $I^k(s,t)$ is the gray value of the pixel (s,t) in k^{th} cell when the center of cell u lies on pixel (i,j). Also, N_{cell} is the number of pixels in each cell. The AAGD algorithm for eight different directions can be computed as:

$$AAGD_k(i,j) = \left(m_0(i,j) - m_k(i,j)\right)^2 \qquad k = 1,\ldots,8 \tag{3}$$

In order to address the hole-like objects issue in AAGD algorithm and reduce false alarms, simply the resulting negative contrast are suppressed using the following thresholding procedure:

$$\begin{aligned} &D_k(i,j) = \\ &AAGD_k(i,j) \times H\left(m_0(i,j) - m_k(i,j)\right) \quad k = 1,\ldots,8 \end{aligned} \tag{4}$$

where $H(\cdot)$ is the Heaviside step function and expressed as:

$$H(x) = \begin{cases} 1 & x \geq 0 \\ 0 & x < 0 \end{cases}. \tag{5}$$

As mentioned before, unlike the structural background clutters, small targets have positive contrast in all directions. Hence, considering minimum directional response as the final output will enhance clutter rejection capability, while the target detection ability remains unchanged. Therefore, in this paper, absolute directional mean difference (ADMD) value is defined as:

$$ADMD(i,j) = \min\left\{D_1(i,j), D_2(i,j), \ldots, D_8(i,j)\right\} \tag{6}$$

This procedure can be done through several scales (cell size) for multi-scale processing. The output of the multi-scale ADMD algorithm can be expressed as:

$$\begin{aligned} &MS\_ADMD(i,j) = \\ &\max\left\{ADMD^1(i,j), ADMD^2(i,j), \ldots, ADMD^S(i,j)\right\} \end{aligned} \tag{7}$$

where $ADMD^s$ denotes the ADMD output at the s^{th} scale.

3.1. Clutter rejection mechanism

Fig. 3 shows the output response of the AAGD, as well as the proposed algorithm, to an infrared scene including a sharp cloud edge, which the gray intensity of all images are normalized to $[0-255]$ interval. As shown in the figure, the proposed algorithm effectively eliminates the high-intensity edge. The gray intensity of the red rectangle does not exceed 0.6 (Fig. 3f). However, the AAGD algorithm has relatively strong response in that area which is demonstrated as two parallel lines in the figure.

As shown in Fig. 3e, the maximum gray intensity of the area related to the red rectangle is about 60 which is approximately 100 times greater than the ADMD output.

In order to investigate the behavior of both AAGD and ADMD algorithms facing sharp edges, a brief analysis is provided here (Fig. 4). Without losing generality, let assume that the area under test just has two gray levels (g_b and g_d values for bright and dark areas, respectively). Also, let assume that both target and background windows are identical for both algorithms. As the final assumption, let assume that the algorithms are constructed just in a single scale. In the first scenario (Fig. 4a), the target window completely lies on bright area. In this situation, the output of the AAGD algorithm can be calculated as:

$$\begin{aligned} out_{AAGD} &= \left(g_b - \left(\frac{5 \times g_b + 3 \times g_d}{8} \right) \right)^2 \\ &= \left(\frac{3}{8} \left(g_b - g_d \right) \right)^2 = \frac{9}{64} \Delta g^2 \end{aligned} \tag{8}$$

According to Eq. 8, as Δg increases (the edge becomes more sharper), the output of the AAGD algorithm becomes more intensified (Fig. 3e).

Considering Fig. 4a as the input scenario, there are only two types of directional output in ADMD algorithm. D_b for the directions along with bright background cells and D_d for the directions along with dark background cells. These two outputs are calculated as follows:

$$\begin{aligned} D_b &= H\left(g_b - g_b \right) \times \left(g_b - g_b \right)^2 = 0 \\ D_d &= H\left(g_b - g_d \right) \times \left(g_b - g_d \right)^2 = \Delta g^2 \end{aligned} \tag{9}$$

Therefore,

$$out_{ADMD} = \min\left\{ D_b, D_d \right\} = \min\left\{ 0, \Delta g^2 \right\} = 0 \tag{10}$$

When the target window has negative contrast compare to the bright background cells (Fig. 4b), the output of AAGD algorithm is computed as follows:

$$\begin{aligned} out_{AAGD} &= \left(g_d - \left(\frac{3 \times g_b + 5 \times g_d}{8} \right) \right)^2 \\ &= \left(\frac{3}{8} \left(g_d - g_b \right) \right)^2 = \frac{9}{64} \Delta g^2 \end{aligned} \tag{11}$$

Eq. 11 demonstrates that, similar to the former scenario (Fig. 4a), the AAGD algorithm returns a strong response for the non-target area. When the center of the target window exactly lies on the edge, the AAGD output takes zero value. This is why there is a dark area between two parallel lines

in the AAGD output (Fig. 3b).

The output of the ADMD algorithm to Fig. 4b scenario is expressed as:

$$\begin{aligned} D_b &= H\left(g_d - g_b\right) \times \left(g_d - g_b\right)^2 = 0 \\ D_d &= H\left(g_d - g_d\right) \times \left(g_d - g_d\right)^2 = 0 \end{aligned} \tag{12}$$

Therefore,

$$out_{ADMD} = \min\left\{D_b, D_d\right\} = \min\left\{0, 0\right\} = 0 \tag{13}$$

According to eqs. (10) and (13), one can conclude that the proposed algorithm effectively eliminates high-intensity edges. It is worth to mention that since the small target has positive contrast in all directions, minimum selection strategy does not degrade detection ability.

3.2. Efficient implementation

In order to construct a single-scale ADMD algorithm, eight directional AAGD algorithm should be computed, separately. Performing these amount of operations needs high processing resources. In this section, the proposed algorithm is reformulated to reduce computational complexity.

Since structural background clutters do not have positive contrast in all directions, considering the maximum average intensity of the background cells in contrast function formulation will mimic the behavior of the proposed algorithm. Therefore,maximum directional mean value M_{dir} is defined as:

$$M_{dir}(i,j) = \max\left\{m_1(i,j), m_2(i,j), \ldots, m_8(i,j)\right\} \tag{14}$$

Accordingly, absolute difference mean value for the pixel (i, j) is calculated as follows:

$$ADM(i,j) = \left(m_0(i,j) - M_{dir}(i,j)\right)^2 \tag{15}$$

By discarding negative values through thresholding operation, the final ADMD output will achieve:

$$ADMD(i,j) = ADM(i,j) \times H\left(m_0(i,j) - M_{dir}(i,j)\right) \tag{16}$$

This new formulation can be efficiently implemented via local averaging and morphology dilation operators. To this end, the following procedure can be utilized to obtain the final saliency map:

1. The input infrared images is filtered using local averaging with proper neighborhood size (3×3, 5×5, 7×7 or 9×9), m_0.
2. The filtered image, m_0, is morphologically dilated using proper structural element (e.g. Fig. 5) to obtain maximum directional value, M_{dir}.

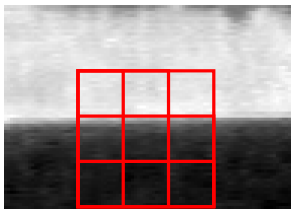

(b)

Figure 4: Two different scenarios to explain AAGD deficiency: **a)** the target window has positive contrast, **b)** the target window has negative contrast.

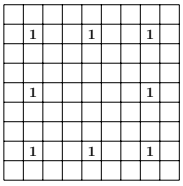

Figure 5: A 9×9 structural element to obtain maximum directional value for 3×3 target size (empty cells have zero values).

3. Then, The absolute difference mean is calculated, ADM.

4. Finally, saliency map is constructed by eliminating negative contrasts, $ADMD$.

Table 1: SCR values for the test targets

	AAGD	TopHat	LCM	PCM	LoG	**ADMD**
Fig. 6a	4.37	1.94	1.55	3.78	2.43	**86.23**
Fig. 6h	9.07	7.17	1.78	3.01	7.27	**22.85**
Fig. 6o	17.31	10.62	2.32	17.14	12.56	**22.65**
Fig. 6v	11.59	3.14	2.29	8.09	5.25	**11.96**
Fig. 6ac	10.87	2.46	2.25	7.34	4.59	**197.28**
Fig. 6aj	13.69	5.22	1.66	6.23	6.95	**549.18**

Table 2: BSF values for the test images

	AAGD	TopHat	LCM	PCM	LoG	**ADMD**
Fig. 6a	8.66	3.36	1.29	5.41	4.00	**114.23**
Fig. 6h	1.89	1.09	0.75	1.77	1.43	**14.77**
Fig. 6o	14.27	2.93	1.05	16.06	4.17	**25.09**
Fig. 6v	2.36	0.26	0.16	1.47	0.46	**3.44**
Fig. 6ac	4.88	0.55	0.29	1.81	0.85	**25.01**
Fig. 6aj	11.59	0.89	0.38	3.52	1.44	**45.29**

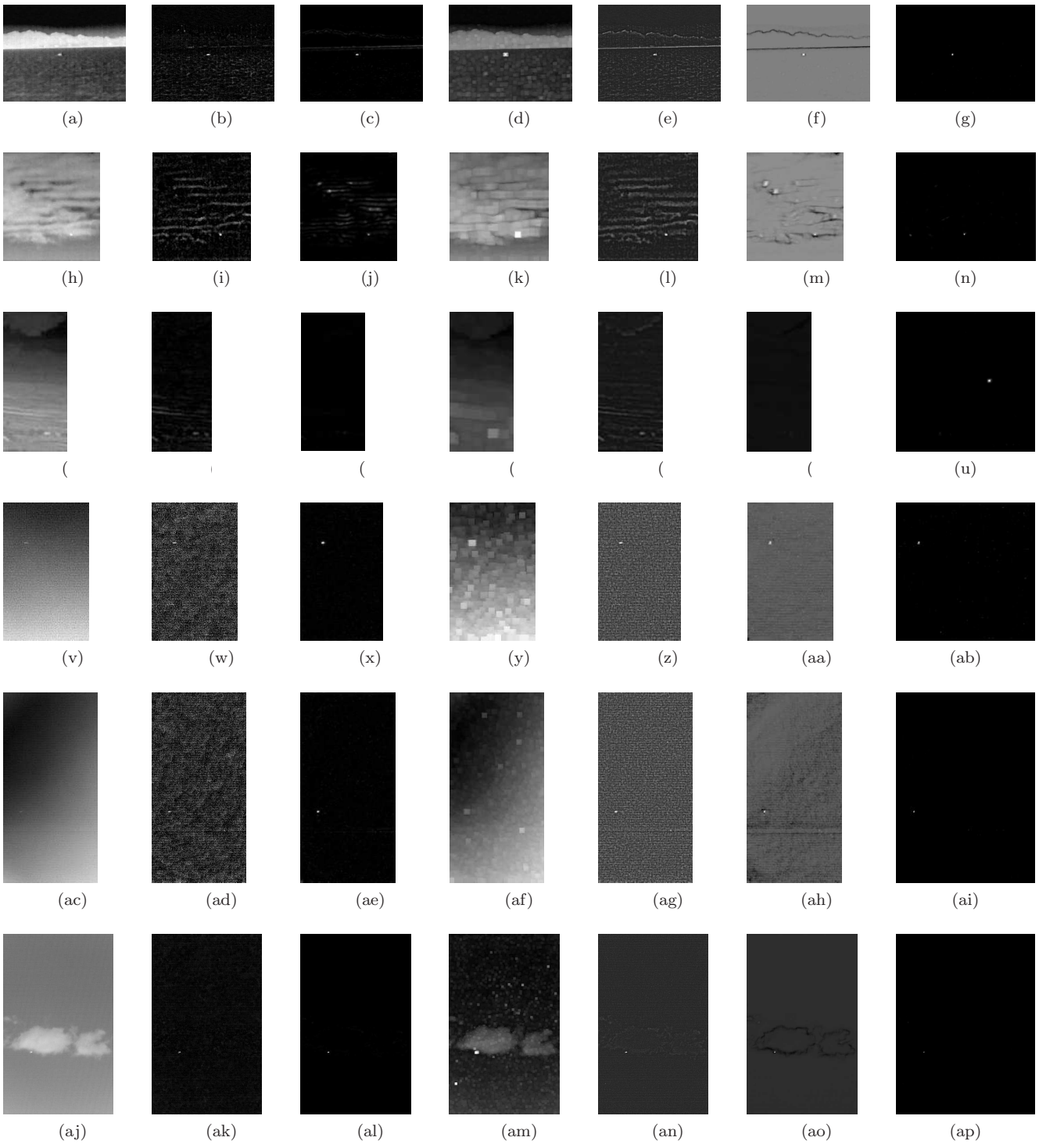

Figure 6: pre-thresholding filtering results on the infrared images. **a, h, o, v, ac, aj)** original images , **b, i, p, w, ad, ak)** filtering results of Top-Hat, **c, j, q, x, ae, al)** filtering results of AAGD, **d, k, r, y, af, am)** filtering results of LCM, **e, l, s, z, ag, an)** filtering results of LoG, **f, m, t, aa, ah , ao)** filtering results of PCM, **g, n, u, ab, ai , ap)** filtering results of **the proposed algorithm** (**ADMD**).

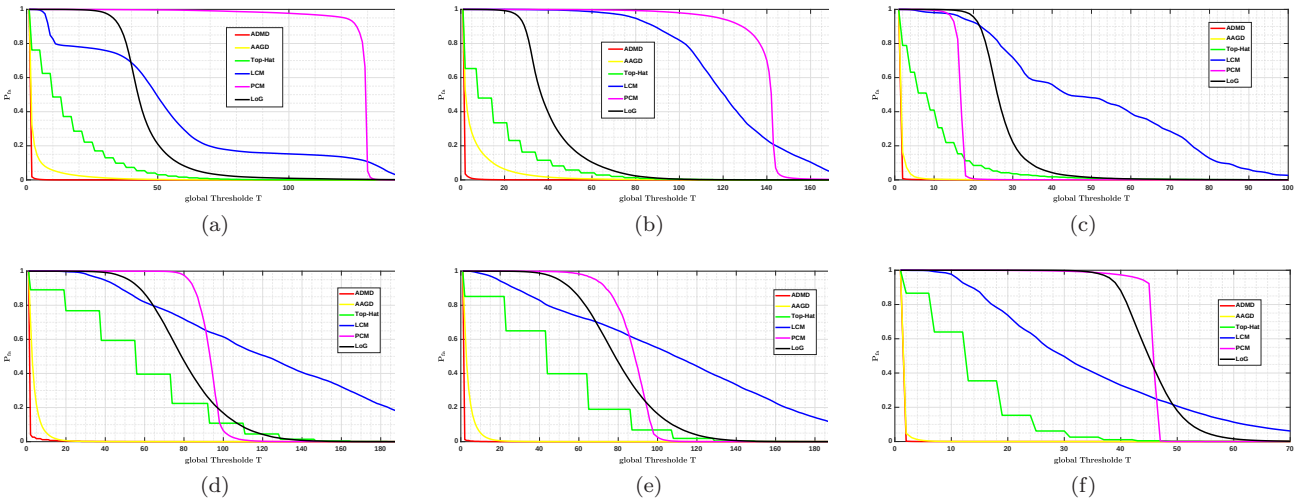

Figure 7: false alarm rate versus threshold level curves for the different test images including: **a)** Fig. 6a, **b)** Fig. 6h, **c)** Fig. 6o, **d)** Fig. 6v, **e)** Fig. 6ac and **f)** Fig. 6aj.

4. Simulation results

4.1. Detection ability analysis

In order to demonstrate the effectiveness of the proposed small target detection algorithm, simulation results are provided here. To compare detection performances, some basic as well as state of the art algorithms like as Top-Hat [6], Laplacian of Gaussian (LoG) [15], local contrast measure (LCM) [8], absolute average gray difference (AAGD) [9] and patch-based contrast measure (PCM) [10] are chosen as baseline algorithms. Except MS-LoG, which uses 12 scales[7], the rest of the algorithms (AAGD, LCM, PCM, and ADMD) utilize four scales. Typically, an small target occupies less than 80 pixels [8], therefore the target window in AAGD as well as the cell size in LCM and PCM take $[3\times 3,\ 5\times 5,\ 7\times 7,\ 9\times 9]$ values to cover different size of the small target. The test images include naval and aerial infrared targets embedded in complicated backgrounds (Fig. 6). The filtering results of the baseline algorithms as well as the proposed one are illustrated in Fig. 6. As shown in the figure, the proposed algorithm (ADMD) effectively suppresses background clutter and enhances the small infrared target while the other methods show poor performances facing these scenarios. Note that, when the input image just contains homogeneous background plus detector noise (Fig. 6v), since there is no structural texture, the performance of the AAGD algorithm is close to the proposed algorithm.

Background suppression factor (BSF) and signal to clutter ratio (SCR) which are defined as follows are used as quantitative measures:

$$BSF = \frac{\sigma_{in}}{\sigma_{out}}, \qquad SCR = \frac{f_T - f_b}{\sigma_b} \tag{17}$$

where f_T, f_b, σ_b, σ_{in} and σ_{out} denote average value of target pixels, mean of background region,

standard deviation of local background, standard deviation of non-target area in original image and standard deviation of non-target area in filtered image, respectively. Higher BSF value indicates better background clutter rejection and the more SCR the more possibility to hit true target. These values are reported in Tab. 1 and Tab. 2 for the test images. As reported in the tables, it is clear that the ADMD algorithm strongly outperforms other methods from both SCR and BSF points of view.

While BSF and SCR are pre-thresholding metrics, false-alarm rate (P_{fa}) is used to evaluate post-thresholding clutter rejection ability

$$P_{fa} = \frac{N_f}{N_w} \tag{18}$$

where N_f and N_w are the number of false alarms and number of all pixels in the whole image, respectively [16]. False-alarm rates versus global threshold level for the test images are shown in Fig. 7. As depicted in the figure, the proposed algorithm has the lowest false-alarm rate compare to the other algorithms. This means that the proposed algorithm effectively suppresses background clutter.

4.2. Execution time analysis

In this section, run-time analysis of the different algorithms are provided to demonstrate the computational complexity of each algorithm. All the algorithms are implemented using OpenCV C++ libraries. The full specifications of the implementation environment are reported in Tab. 3. Each detection algorithm is executed 100 times and the average execution time for the multi-scale (except MS-LoG algorithm which utilizes 12 scales [7], the other multi-scale algorithms consist of four identical scales) as well as the single-scale versions of the algorithms are reported in Tab. 4 and Tab. 5, respectively. AS reported in the Tab. 4, the efficient implementation of the ADMD algorithm (ADMD_{eff}) is almost 27 times faster than the original ADMD. Since the whole 288×110000 panorama image is captured every 1.5 second, none of these multi-scale algorithms can operate in real-time using the reported hardware (Tab. 3). GPU implementation will be a good choice for real-time implementation of these algorithms. Tab. 5 shows the average execution time for single-scale algorithms. As reported in the table, TopHat, AAGD and ADMD_{eff} algorithms can be implemented in real-time using the reported hardware. Also, it can be clearly seen that the efficient ADMD_{eff} algorithm is significantly faster than the original ADMD algorithm.

5. Conclusion

Infrared small target detection is of great importance in a wide range of applications such as surveillance, remote sensing, security and astronomy. Despite the high attention paid to this filed, the lack

of robust and effective target detection method is tangible. To develop a robust small target detection algorithm, in this paper, a directional approach is constructed for better background suppression. Since the small targets have positive local contrast in all directions, in the proposed method, the maximum background intensity (or the minimum local difference) is adopted in absolute average gray difference (AAGD) algorithm. The proposed method effectively suppresses the high-intensity edges and structural background clutters, while the noise suppression and target enhancement ability remain undegraded. In the next step, an efficient implementation procedure is provided using specific structural elements. The simulation results on different real scenarios prove the significant performance and remarkable effectiveness of the proposed method.

References

[1] S. Türker-Kaya, C. W. Huck, A review of mid-infrared and near-infrared imaging: principles, concepts and applications in plant tissue analysis, Molecules 22 (1) (2017) 168.

[2] X. Jin, J. Li, T. J. Schmit, M. D. Goldberg, Evaluation of radiative transfer models in atmospheric profiling with broadband infrared radiance measurements, International journal of remote sensing 32 (3) (2011) 863–874.

[3] D. Liu, L. Cao, Z. Li, T. Liu, P. Che, Infrared small target detection based on flux density and direction diversity in gradient vector field, IEEE Journal of Selected Topics in Applied Earth Observations and Remote Sensing (99) (2018) 1–27.

[4] P. Khaledian, S. Moradi, E. Khaledian, A new method for detecting variable-size infrared targets, in: Sixth International Conference on Digital Image Processing, International Society for Optics and Photonics, 2014, pp. 91591J–91591J.

[5] S. D. Deshpande, M. H. Er, R. Venkateswarlu, P. Chan, Max-mean and max-median filters for detection of small targets, in: Signal and Data Processing of Small Targets 1999, Vol. 3809, International Society for Optics and Photonics, 1999, pp. 74–84.

Table 3: The full specifications of the implementation environment

Operating System	Linux (Ubuntu 18.04, X64)
Linux kernel version	4.15.0-42-generic
OpenCV version	3.4.3
Compiler	GCC 7.3.0
Size of the test image	288×5600
data depth and type	single channel 32 bit floating point
CPU	Intel CORE i7-3520M @ 2.90GHz
Memory	8GB DDR3 @ 1600MHz

Table 4: The average execution time for ***multi-scale*** algorithms. ADMD_{eff} denotes efficient implementation of the ADMD algorithm.

Detection method	**execution time (mS)**
AAGD	145.323
LCM	4555.747
LoG	213.667
PCM	3463.643
ADMD	4612.893
ADMD_{eff}	171.893

Table 5: The average execution time for ***single-scale*** algorithms. ADMD_{eff} denotes efficient implementation of the ADMD algorithm.

Detection method	**execution time (mS)**
AAGD, 7×7 target window	40.622
LCM, 7×7 cell size	1111.990
TopHat, 7×7 flat SE	4.536
PCM, 7×7 cell size	1040.885
ADMD, 9×9 cell size	1195.462
ADMD, 7×7 cell size	1125.827
ADMD, 5×5 cell size	1109.403
ADMD_{eff}, 9×9 cell size	63.002
ADMD_{eff}, 7×7 cell size	46.405
ADMD_{eff}, 5×5 cell size	32.049

[6] M. Zeng, J. Li, Z. Peng, The design of top-hat morphological filter and application to infrared target detection, Infrared Physics & Technology 48 (1) (2006) 67–76.

[7] S. Kim, J. Lee, Scale invariant small target detection by optimizing signal-to-clutter ratio in heterogeneous background for infrared search and track, Pattern Recognition 45 (1) (2012) 393–406.

[8] C. P. Chen, H. Li, Y. Wei, T. Xia, Y. Y. Tang, A local contrast method for small infrared target detection, IEEE Transactions on Geoscience and Remote Sensing 52 (1) (2014) 574–581.

[9] H. Deng, X. Sun, M. Liu, C. Ye, X. Zhou, Infrared small-target detection using multiscale gray difference weighted image entropy, IEEE Transactions on Aerospace and Electronic Systems 52 (1) (2016) 60–72.

[10] Y. Wei, X. You, H. Li, Multiscale patch-based contrast measure for small infrared target detection, Pattern Recognition 58 (2016) 216–226.

[11] S. Moradi, P. Moallem, M. F. Sabahi, A false-alarm aware methodology to develop robust and efficient multi-scale infrared small target detection algorithm, Infrared Physics & Technology 89 (2018) 387–397.

[12] S. Qi, J. Ma, C. Tao, C. Yang, J. Tian, A robust directional saliency-based method for infrared small-target detection under various complex backgrounds, IEEE Geoscience and Remote Sensing Letters 10 (3) (2013) 495–499.

[13] C. Yang, J. Ma, S. Qi, J. Tian, S. Zheng, X. Tian, Directional support value of gaussian transformation for infrared small target detection, Applied optics 54 (9) (2015) 2255–2265.

[14] X. Zhang, Q. Ding, H. Luo, B. Hui, Z. Chang, J. Zhang, Infrared small target detection based on directional zero-crossing measure, Infrared Physics & Technology 87 (2017) 113–123.

[15] S. Kim, J.-H. Lee, Robust scale invariant target detection using the scale-space theory and optimization for irst, Pattern analysis and applications 14 (1) (2011) 57–66.

[16] S. Moradi, P. Moallem, M. F. Sabahi, Scale-space point spread function based framework to boost infrared target detection algorithms, Infrared Physics & Technology 77 (2016) 27–34.